DIGITAL ACCESS TO SCHOLARSHIP AT HARVARD
DASH.HARVARD.EDU

HARVARD LIBRARY

Rapid, Single-Cell Analysis and Discovery of Vectored mRNA Transfection In Vivo with a loxP-Flanked tdTomato Reporter Mouse

Citation

Kauffman, Kevin J., Matthias A. Oberli, J. Robert Dorkin, Juan E. Hurtado, James C. Kaczmarek, Shivani Bhadani, Jeff Wyckoff, Robert Langer, Ana Jaklenec, and Daniel G. Anderson. 2017. "Rapid, Single-Cell Analysis and Discovery of Vectored mRNA Transfection In Vivo with a loxP-Flanked tdTomato Reporter Mouse." Molecular Therapy. Nucleic Acids 10 (1): 55-63. doi:10.1016/j.omtn.2017.11.005. http://dx.doi.org/10.1016/j.omtn.2017.11.005.

Published version

https://doi.org/10.1016/j.omtn.2017.11.005

Link

http://nrs.harvard.edu/urn-3:HUL.InstRepos:34651779

Terms of use

This article was downloaded from Harvard University's DASH repository, and is made available under the terms and conditions applicable to Other Posted Material (LAA), as set forth at
https://harvardwiki.atlassian.net/wiki/external/NGY5NDE4ZjgzNTc5NDQzMGIzZWZhMGFlOWI2M2EwYTg

Accessibility

https://accessibility.huit.harvard.edu/digital-accessibility-policy

Share Your Story

The Harvard community has made this article openly available.
Please share how this access benefits you. Submit a story

Molecular Therapy
Nucleic Acids
Original Article

Rapid, Single-Cell Analysis and Discovery of Vectored mRNA Transfection *In Vivo* with a loxP-Flanked tdTomato Reporter Mouse

Kevin J. Kauffman,[1,2,7] Matthias A. Oberli,[1,2,7] J. Robert Dorkin,[2,3] Juan E. Hurtado,[4] James C. Kaczmarek,[1,2] Shivani Bhadani,[2] Jeff Wyckoff,[2] Robert Langer,[1,2,5,6] Ana Jaklenec,[2] and Daniel G. Anderson[1,2,5,6]

[1]Department of Chemical Engineering, Massachusetts Institute of Technology, Cambridge, MA 02139, USA; [2]David H. Koch Institute for Integrative Cancer Research, Massachusetts Institute of Technology, Cambridge, MA 02139, USA; [3]Department of Biology, Massachusetts Institute of Technology, Cambridge, MA 02139, USA; [4]Department of Biological Engineering, Massachusetts Institute of Technology, Cambridge, MA 02139, USA; [5]Institute for Medical Engineering and Science, Massachusetts Institute of Technology, Cambridge, MA 02139, USA; [6]Harvard MIT Division of Health Sciences and Technology, Massachusetts Institute of Technology, Cambridge, MA 02139

mRNA therapeutics hold promise for the treatment of diseases requiring intracellular protein expression and for use in genome editing systems, but mRNA must transfect the desired tissue and cell type to be efficacious. Nanoparticle vectors that deliver the mRNA are often evaluated using mRNA encoding for reporter genes such as firefly luciferase (FLuc); however, single-cell resolution of mRNA expression cannot generally be achieved with FLuc, and, thus, the transfected cell populations cannot be determined without additional steps or experiments. To more rapidly identify which types of cells an mRNA formulation transfects *in vivo*, we describe a Cre recombinase (Cre)-based system that permanently expresses fluorescent tdTomato protein in transfected cells of genetically modified mice. Following *in vivo* application of vectored Cre mRNA, it is possible to visualize successfully transfected cells via Cre-mediated tdTomato expression in bulk tissues and with single-cell resolution. Using this system, we identify previously unknown transfected cell types of an existing mRNA delivery vehicle *in vivo* and also develop a new mRNA formulation capable of transfecting lung endothelial cells. Importantly, the same formulations with mRNA encoding for fluorescent protein delivered to wild-type mice did not produce sufficient signal for any visualization *in vivo*, demonstrating the significantly improved sensitivity of our Cre-based system. We believe that the system described here may facilitate the identification and characterization of mRNA delivery vectors to new tissues and cell types.

INTRODUCTION

mRNA therapeutics have the potential to address unmet medical needs by inducing specific intracellular protein expression *in vivo*. mRNA-based therapies have entered clinical trials for vaccine and protein replacement applications and are being studied pre-clinically in other areas, such as genome editing.[1,2] However, delivery of mRNA into the target tissue and the cytoplasm of the target cell type remains challenging for some tissue types. Various vectors, such as lipid and polymeric nanoparticles, have been utilized to encapsulate and deliver mRNA payloads intracellularly.[3,4] To evaluate the transfection ability, biodistribution, and pharmacokinetics of these delivery vectors *in vivo*, mRNAs coding for reporter genes (e.g., bioluminescent luciferases, fluorescent proteins, β-galactosidase, and others) are often used to optimize the system before therapeutic mRNA delivery is attempted.[5] Additionally, for most vectored mRNA delivery applications, it is useful to identify not only the targeted tissue but also the targeted cell populations within that tissue. For example, cancer immunotherapies would ideally express mRNA encoding antigen in dendritic cells of the lymphatic system;[6,7] conversely, protein replacement therapy for cystic fibrosis would target expression of mRNA encoding CFTR in lung epithelial cells.[8,9]

Firefly luciferase (FLuc) mRNA is a commonly used reporter mRNA in the literature for *in vivo* studies and has been used to demonstrate mRNA transfection in the liver,[10,11] spleen,[12,13] pancreas,[11] lung,[13,14] bone marrow,[13] lymph nodes,[13,15] muscle,[16,17] and xenograft tumors.[18] Upon activation by a nontoxic and stable substrate, FLuc emits light at tissue-penetrating wavelengths that can be imaged *in vivo*,[19] making FLuc useful for surveying the entire animal and identifying mRNA translation in bulk tissues. Thus, this *in vivo* bioluminescence imaging (BLI) technique is a powerful tool to localize protein expression and guide the researcher to the most appropriate tissue for further *in vivo* analysis with fluorescent markers.[20] However, the desired single-cell resolution cannot be achieved with FLuc using conventional techniques such as flow cytometry or microscopy, which require a strong fluorescent signal, without the use of

Received 1 September 2017; accepted 15 November 2017;
https://doi.org/10.1016/j.omtn.2017.11.005.

[7]These authors contributed equally to this work.

Correspondence: Daniel G. Anderson, David H. Koch Institute for Integrative Cancer Research, 500 Main Street, Massachusetts Institute of Technology, Cambridge, MA 02139, USA.
E-mail: dgander@mit.edu

This is an open access article under the CC BY-NC-ND license (http://creativecommons.org/licenses/by-nc-nd/4.0/).

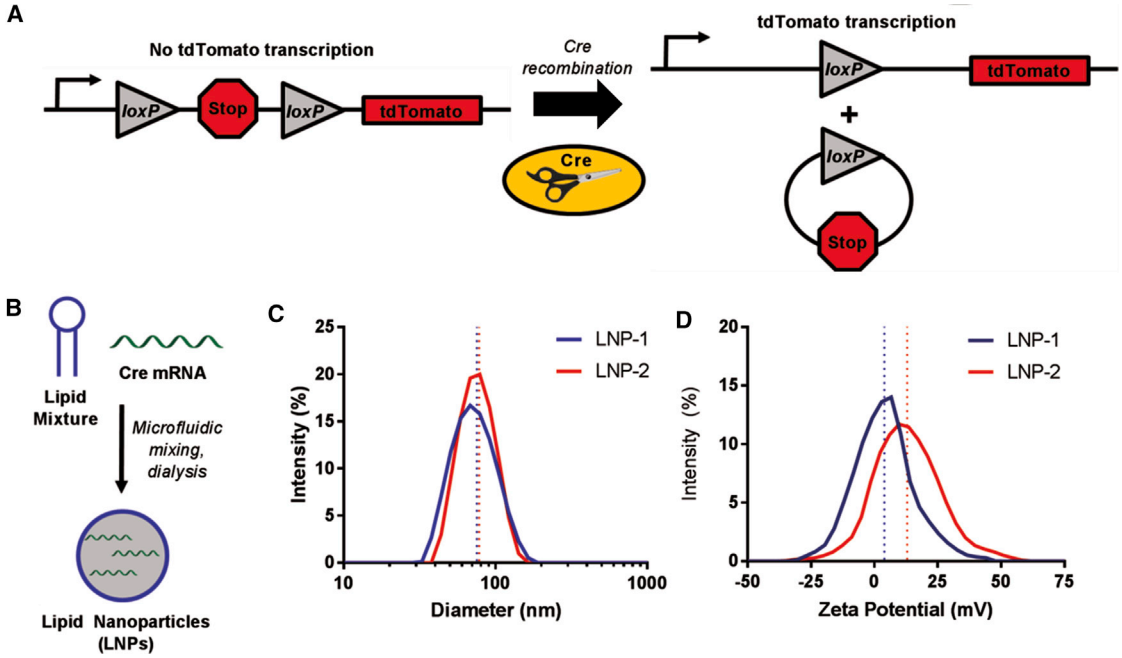

Figure 1. Ai14/Cre mRNA Mouse Model Description and Lipid Nanoparticle Characterization

(A) Diagram of the *loxP*-flanked STOP cassette upstream of tdTomato with and without Cre recombination. (B) Schematic of the LNP formulation process (see a more detailed description in Figure S4). (C) Diameter distribution for LNP-1 and LNP-2. (D) Zeta potential distribution for LNP-1 and LNP-2.

engineered luciferase-fluorescent protein conjugates[21–23] or additional disruptive antibody staining steps requiring membrane permeabilization.[24,25] In principle, mRNAs encoding fluorescent proteins can allow for facile single-cell analysis via microscopy or flow cytometry. However, current commercially available GFP and tdTomato mRNAs delivered to wild-type mice using previously reported formulations and doses did not induce sufficient protein expression to be visualized *in vivo* above background fluorescence despite having strong GFP and tdTomato signals when delivered to cells *in vitro* (Figures S1–S3). Thus, there is a need for a mouse model that can sensitively and rapidly identify mRNA-transfected cell populations *in vivo* to optimize mRNA delivery vectors for diverse cellular targets and clinical applications.

We hypothesized that *in vivo* delivery of mRNA could be more easily visualized in a genetically modified mouse with a loxP-flanked STOP cassette preventing transcription of a CAG promoter-driven tdTomato protein in all cells, such as the Ai14 reporter mouse (Figure 1A).[26] In this model, cells that are successfully transfected with mRNA encoding Cre recombinase (Cre) would excise the loxP-flanked STOP cassette, resulting in permanent tdTomato transcription and subsequent strong, amplified tdTomato expression. To validate this model, we delivered Cre mRNA with two distinct delivery vectors to Ai14 mice and analyzed the resultant tdTomato expression using whole-organ imaging, fluorescence microscopy, and flow cytometry. In this report, we use this Ai14/Cre mRNA mouse model to describe vectored mRNA transfection *in vivo* with single-cell resolution at low mRNA doses.

RESULTS AND DISCUSSION

Validation of the Ai14/Cre mRNA Model *In Vivo*

We first investigated whether vectored mRNA encoding for GFP or tdTomato could result in sufficient GFP or tdTomato signal for whole-organ imaging. An optimized[11] lipid nanoparticle (LNP) formulation (Figures 1B and 1C) capable of achieving high levels of FLuc mRNA expression predominately in the liver following intravenous administration to mice (LNP-1) has been reported previously.[10] The composition of LNP-1 is shown in Figure S4. We formulated LNP-1 with commercially available GFP or tdTomato mRNA and administered it intravenously to wild-type C57BL/6 mice at 0.3 mg/kg. The GFP or tdTomato fluorescence of the liver and two additional organs (spleen and lungs) was measured at 24 hr, the approximate half-life of these fluorescent proteins (Figure 2A).[27] We found no detectable GFP or tdTomato signal from LNP-1-administered wild-type mice at this dose using GFP or tdTomato mRNAs, meaning that an alternative method of measuring mRNA translation in whole organs is needed for LNP-1.

We next tested the ability of the hypothesized Ai14/Cre mRNA model to produce measurable tdTomato expression in whole organs. We formulated Cre mRNA into LNP-1 and administered it intravenously to Ai14 mice at 0.3 mg/kg. 48 hr post-injection (to provide additional time for the Cre recombination and transcription steps), there was tdTomato expression in the liver that was orders of magnitude higher than background tissue autofluorescence (Figure 2A), demonstrating that vectored Cre mRNA could generate a tdTomato signal in Ai14 mice as proposed. Furthermore, the liver biodistribution of tdTomato

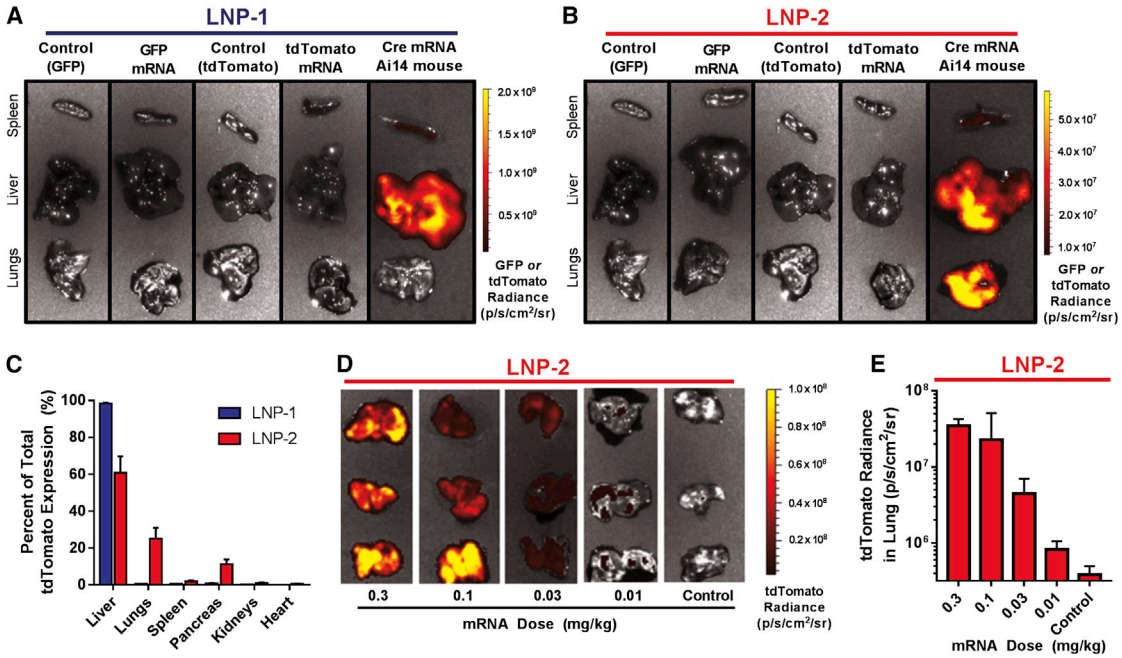

Figure 2. Whole-Organ Fluorescence for the Ai14/Cre mRNA Mouse Model

(A and B) Representative (n = 3, 1 pictured) GFP or tdTomato expression in three organs for (A) LNP-1- or (B) LNP-2-injected mice under IVIS imaging. LNPs with GFP and tdTomato mRNA were administered to C57BL/6 mice (24 hr), and LNPs with Cre mRNA were administered to Ai14 mice (48 hr). Control mice are PBS-treated C57BL/6 mice. (C) Biodistribution of tdTomato fluorescence for LNP-1 and LNP-2 in Ai14 mice. (D) tdTomato expression in the lungs for LNP-2 in Ai14 mice at various doses under IVIS imaging. (E) Quantification of (D). The data in (C) and (E) are presented as mean + SD, n = 3.

expression was comparable with that of previously published[10] Luc expression (Figure S5) for LNP-1, suggesting that the Ai14/Cre mRNA model can successfully describe the whole-organ expression of protein from vectored mRNA.

Characterization of a New Formulation with Whole-Organ Imaging

Recently, a publication by Kranz et al.[13] reported that FLuc-encoding mRNA-LNPs could be redirected to the lungs by increasing the zeta potential of the LNP. To this end, we sought to formulate a new, more positively charged version of our LNP (LNP-2) and examine its tissue delivery properties (Figure 1D; Figure S4). As hypothesized, intravenous administration of LNP-2 encapsulating Cre mRNA to Ai14 mice resulted in significant tdTomato expression in the lungs (Figures 2B and 2C), consistent with the related formulation and data generated described by Kranz et al.[13] with FLuc mRNA. As previously observed with LNP-1, no observable whole-organ fluorescence was found in C57BL/6 mice administered LNP-2 formulated with GFP or tdTomato mRNA at a 0.3 mg/kg (approximately 5 μg) dose (Figure 2B). To test the sensitivity of our Ai14/Cre mRNA model, we performed a dose-response experiment with LNP-2 in the lungs and detected tdTomato expression by IVIS at mRNA doses as low as 0.01 mg/kg (approximately 200 ng) (Figures 2D and 2E) Importantly, tdTomato expression was dose-dependent, suggesting that tdTomato expression can be used both as a proxy for vectored mRNA transfection efficacy and to potentially estimate the percentage of transfected cells in a given tissue.

Two-Photon Microscopy for the Ai14/Cre mRNA Model

One potential advantage of the Ai14/Cre mRNA model over traditional FLuc reporter models is the ability to rapidly perform fluorescence microscopy to probe the cellular structure of tdTomato-expressing tissues and flow cytometry to identify tdTomato-expressing cell populations. Although FLuc would require additional secondary antibody staining (which is also more disruptive for intracellular proteins like FLuc because of the need to permeabilize the cellular membrane), tdTomato-expressing tissues and cells from Ai14 mice can be immediately analyzed. We chose to first perform two-photon excitation microscopy because it uses freshly isolated tissue and requires no potentially damaging fixation or lengthy antibody staining steps.[28] This technique was used to study the liver, spleen, and lung tissue architecture of LNP-1- and LNP-2-administered Ai14 mice (Figure 3), revealing tdTomato expression in liver cells (Figure 3A), spleen cells (Figure 3B), and cells lining both exterior (Figure 3C) and interior (Figure 3D) blood vessels of the lung.

Microscopy experiments for LNP-1 injected Ai14 mice revealed tdTomato expression in liver cells (Figure 3A). We postulate these tdTomato$^+$ cells to be hepatocytes because their morphology is cuboidal,[29] and previous small interfering RNA (siRNA) formulations made with LNPs similar to LNP-1 were found to silence expression of a hepatocyte-specific protein *in vivo*.[30] The spleen (Figure 3B) has a high degree of autofluorescence because of the abundance of phagocytic cells that endocytose autofluorescent debris and dead cells,

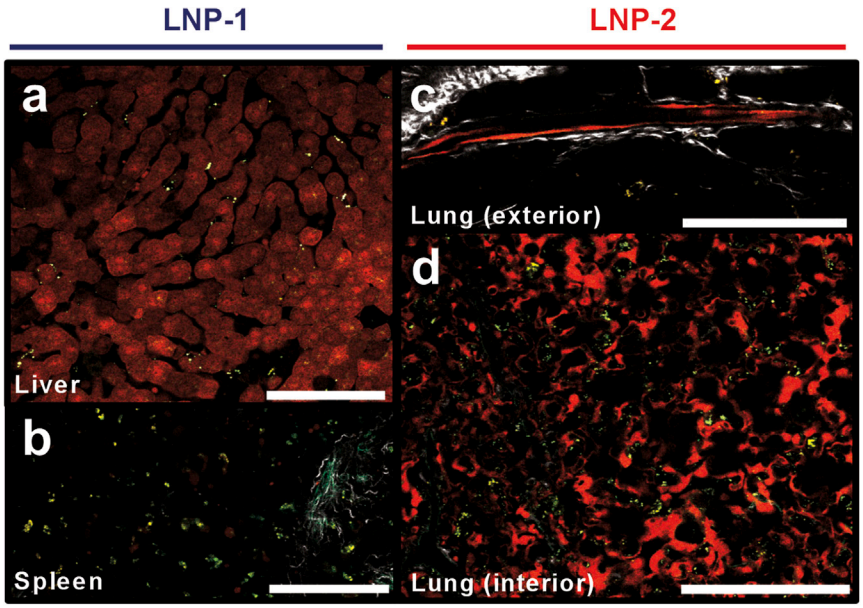

Figure 3. Two-Photon Excitation Microscopy of Tissues for the Ai14/Cre mRNA Mouse Model
(A) Liver cells treated with LNP-1. (B) Spleen cells treated with LNP-1. (C) Blood vessel on the exterior of a lung treated with LNP-2. (D) Interior of a lung treated with LNP-2. Scale bars, 100 μm. Gray, collagen I (emission wavelength [Em.] 425/30 nm); green, tissue autofluorescence (Em. 525/45 nm); red, tdTomato (Em. 607/70 nm).

but tdTomato$^+$ cells are still clearly visible. For LNP-2-administered Ai14 mice, we observed tdTomato$^+$ cells that lined exterior blood vessels of the lungs (Figure 3C) and tdTomato$^+$ cells in the interior of the lungs in the blood vessels surrounding the alveoli (Figure 3D). To more conclusively identify these transfected lung and spleen cell populations, flow cytometry was performed next.

Flow Cytometry of Lung-Targeting Formulations

We then investigated the ability of lung cells isolated from the LNP-2-administered Ai14 mice to undergo flow cytometry. As observed for whole-organ imaging, flow cytometry analysis could not detect GFP or tdTomato fluorescence above background for wild-type mice administered LNP-2 formulated with GFP or tdTomato mRNA (Figure 4A). However, a strong tdTomato signal was observed in CD31$^+$ (endothelial) cells of the lung for Ai14 mice administered LNP-2 formulated with Cre mRNA (Figure 4A). A 2D plot of CD31 versus tdTomato for all lung cells confirmed that tdTomato-positive cells were nearly exclusively CD31$^+$ (endothelial) lung cells (Figure 4B), with over 75% of isolated CD31$^+$ lung cells expressing tdTomato at the highest tested dose (0.3 mg/kg) (Figure 4C). At the lowest dose tested (0.01 mg/kg), our Ai14/Cre mRNA model could still clearly identify a tdTomato$^+$ population comprising only 0.4% of all CD31$^+$ lung cells.

Kranz et al.[13] previously reported that mRNA-LNPs could be redirected to the lungs by increasing their cationic character but did not identify which cell types were transfected. For the first time, we identify endothelial cells as the primary transfected lung cell population when mice are administered LNP-2, a newly described, more cationic version of LNP-1, using two methods of detection (Figures 3 and 4). The observation of endothelial cell targeting by cationic LNPs matches reports of previous lung-targeting siRNA-based cationic formulations that silenced protein expression in lung endothelial cells but not epithelial or immune cell populations in the lung.[31,32] The ability to selectively transfect lung endothelial cells with therapeutic mRNAs is important for many clinical applications, including pulmonary hypertension[33] and cancer.[34]

Flow Cytometry to Identify Rare Populations in the Spleen

We next aimed to compare the efficacy of two mRNA delivery vectors in a more complex population of cells; furthermore, we sought to identify rarer transfected cell populations that would challenge the sensitivity of the Ai14/Cre mRNA model for visualization. We chose to study the immune cell population of the spleen because LNP-1 and LNP-2 were both identified to weakly transfect spleen cells (Figures 2A and 2B), and the spleen contains a variety of therapeutically important immune cells involved in both the innate and adaptive immune responses.[35] Although a majority of lung CD31$^+$ cells expressed tdTomato in LNP-2-treated mice, CD45$^+$ spleen cells expressing tdTomato in LNP-1-treated mice are much less common (Figure 5A) and only observable in the Cre/Ai14 mouse model.

Flow cytometry analysis of Ai14 mice administered LNP-1 and LNP-2 identified a wide variety of tdTomato$^+$ spleen immune cells (Figure 5B). Notably, LNP-1 resulted in greater proportions of all measured tdTomato$^+$ splenic CD45$^+$ populations compared with LNP-2, matching the observation that whole-spleen tdTomato fluorescence is significantly greater for LNP-1 than LNP-2 (Figures 2A and 2B; Figure S6). Compared with other CD45$^+$ cells, both LNP-1 and LNP-2 transfected a greater proportion of macrophages (CD11b$^+$, F4/80$^+$) than any other cell type. Although macrophages made up less than 1% of CD45$^+$ cells, they accounted for approximately 25% of the total tdTomato$^+$ CD45$^+$ cells in the spleen (Figure 5C).

siRNA-formulated lipid nanoparticles similar in composition to LNP-1 have been found previously to silence protein predominately in hepatocytes with only weak silencing in splenic myeloid cells.[30] However, no further transfected splenic cell types were identified with siRNA, and the ability of LNP-1-type formulations to transfect splenic cells with mRNA has not yet been investigated. In the present study, with mRNA-formulated LNP-1 vectors in the Ai14/Cre mRNA model, we discovered many additional splenic cell types with clearly identifiable mRNA-induced tdTomato$^+$ populations.

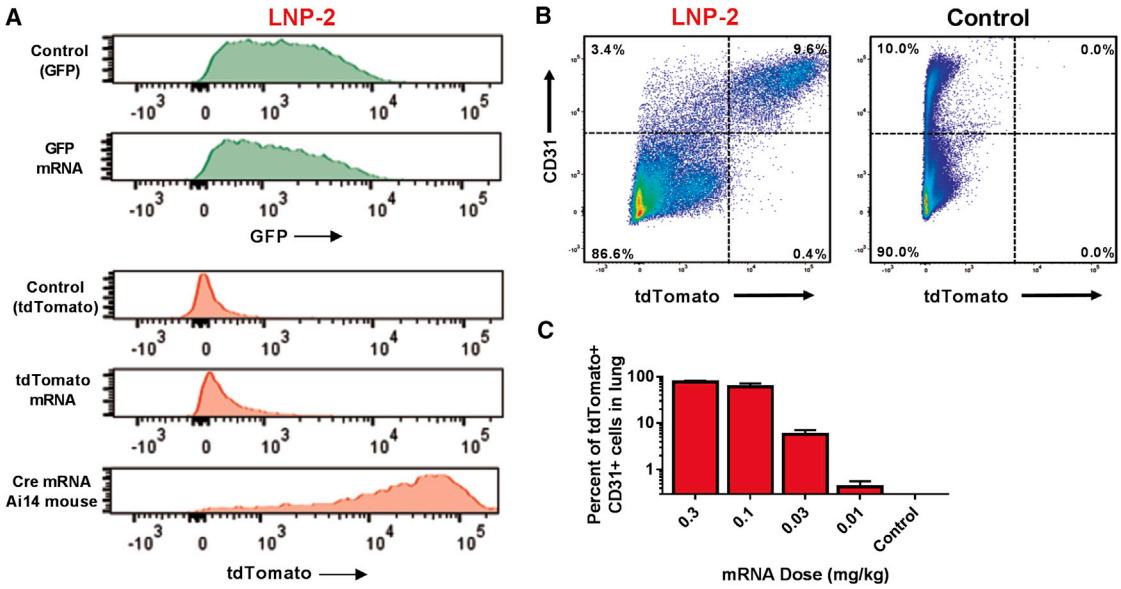

Figure 4. Single-Cell Analysis of Lung Cells from the Ai14/Cre mRNA Mouse Model

(A) Representative (n = 3, 1 pictured) histograms of GFP or tdTomato signal for CD31$^+$ (endothelial) lung cells in LNP-2-administered mice, determined by flow cytometry. LNPs with GFP and tdTomato mRNA were administered to C57BL/6 mice (24 hr), and LNPs with Cre mRNA were administered to Ai14 mice (48 hr). Control mice are PBS-treated C57BL/6 mice. (B) Representative fluorescence-activated cell sorting (FACS) plot of lung CD31 versus tdTomato for LNP-2-injected (left) and control-injected (right) mice. (C) Percent of lung CD31$^+$ cells that are tdTomato$^+$ at multiple doses in LNP-2-injected Ai14 mice, presented as mean + SD, n = 3.

Excitingly, LNP-1 promoted mRNA expression in many cell types important for mRNA immunotherapies,[6,35] including lymphocytes and antigen-presenting cells (Figure 5) with approximately 4% of splenic dendritic cells and over half of macrophages transfected, making LNP-1 an attractive candidate for future studies with mRNA-based vaccines or immuno-modulators. It should be noted that, although tdTomato expression was observed in a wide variety of differentiated immune cells in the spleen at the time of isolation, we cannot rule out the possibility that such cells were progenitor cells or circulating immune cells at the time of transfection, and, thus, the number of transfected cells may be over-estimated.

The discovery of these transfected cell types *in vivo* would not have been possible or would have required significantly more labor with vectored siRNA. It has been common practice to determine whether siRNA vectors were efficacious in particular cell types by designing siRNA against proteins only expressed in those cells (e.g., Factor VII for hepatocytes[30,36,37] and Tie2 for endothelial cells[31,32]); mRNA offers no such analog because any cell with the proper ribosomal machinery should, in principle, be capable of translation. Many delivery vectors originally designed for siRNA delivery have been re-engineered for mRNA delivery.[3] The identification of many new cell populations successfully transfected by mRNA vectors like LNP-1 and LNP-2 suggests that, unless the mRNA versus siRNA payload dramatically affects vector transfection ability, siRNA vectors may have been transfecting more cell types than originally thought and may have been limited in efficacy only by siRNA potency.

Comparison of the Ai14/Cre mRNA Model with Other Systems

Many potential mRNA therapies could benefit from formulations capable of providing selective delivery to the required tissue and cell type *in vivo*. Different mRNA imaging methods provide for different levels of sensitivity. One of the most common reporters for surveying *in vivo* mRNA activity is FLuc mRNA, which, when translated into protein and activated by substrate, emits measurable light. However, identification of transfected cell populations by FLuc is challenging because immunohistochemistry or flow cytometry would require incubation with secondary anti-FLuc fluorescently tagged antibodies that must permeabilize and potentially disrupt the cellular membrane.[38] Because of these challenges, alternate approaches have often been taken. For example, two independent reports confirmed the transfection of splenic CD11c$^+$ cells with an mRNA vector by comparing FLuc expression between wild-type and genetically modified CD11c-depleted mice;[13,39] however, this generalized approach would require a different knockout mouse for every potential transfected cell type of interest, which researchers would also need to know *a priori*.

Alternatively, some publications have used fluorophore-labeled RNAs *in vivo* to study the biodistribution and cellular localization of vectored nucleic acids.[14,32,40,41] However, tissue and cellular transfection of the mRNA itself does not always correlate well with translation of the desired protein.[14] Furthermore, this method cannot distinguish between fluorophore-labeled mRNA adhered to the surface of cells, those that are trapped in cellular compartments such as endosomes, and those that have successfully transfected into the

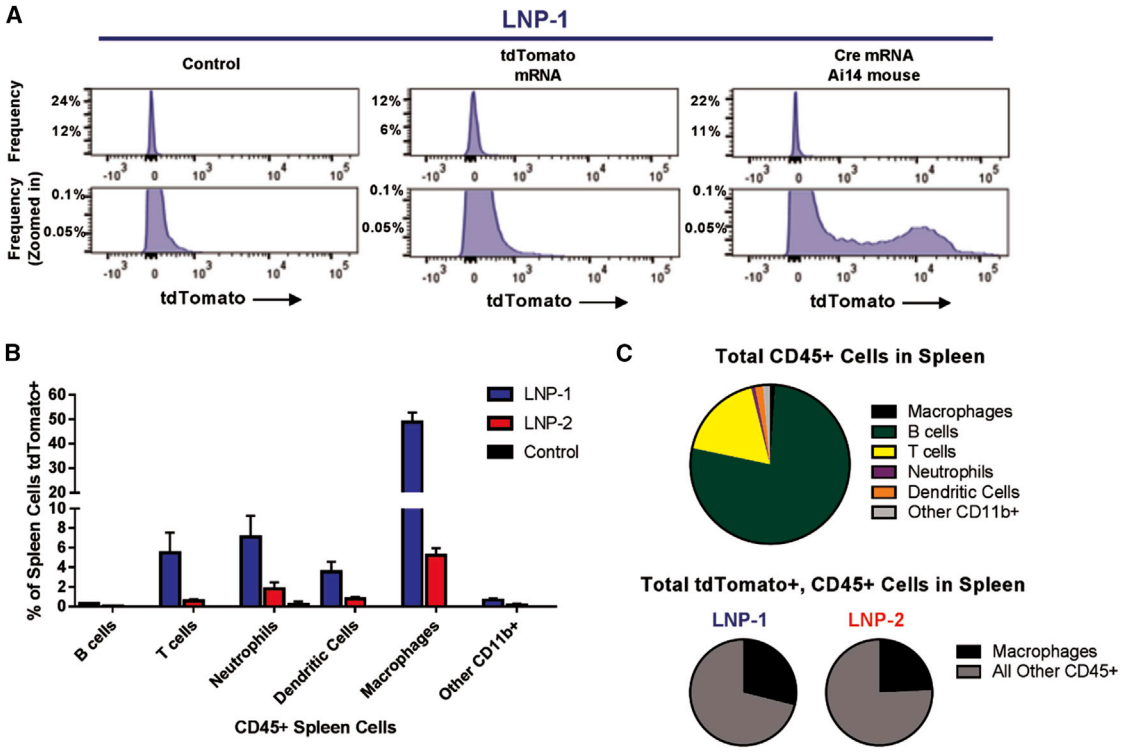

Figure 5. Single-Cell Analysis of Spleen Cells from the Ai14/Cre mRNA Mouse Model

(A) Representative (n = 3, 1 pictured) histograms of tdTomato signal for CD45$^+$ (immune) spleen cells in LNP-1-administered mice, determined by flow cytometry. The y axis on the histograms in the bottom row is enlarged to highlight the tdTomato signal. LNPs with GFP and tdTomato mRNA were administered to C57BL/6 mice, and LNPs with Cre mRNA were administered to Ai14 mice. Control mice are PBS-treated C57BL/6 mice. (B) Percent of CD45$^+$ spleen cells that are tdTomato$^+$ in LNP-1- or LNP-2-injected Ai14 mice, presented as mean + SD, n = 3. (C) Distribution of CD45$^+$ splenic cells (top) and tdTomato$^+$ CD45$^+$ splenic cells (bottom), presented as mean, n = 3.

cytoplasm. Because knowing the biodistribution of mRNA and vector materials is indeed important for understanding both toxicity and pharmacokinetics, the use of fluorophore-labeled mRNA vectors in concert with the Ai14/Cre mRNA model would give a more complete description of the *in vivo* behavior of mRNA delivery vectors.

In this report, we present a mouse model to determine the location of mRNA expression *in vivo* with single-cell resolution using commercially available reagents and mice. Using previously reported and novel lipid nanoparticle vectors, we deliver mRNA encoding for Cre protein to Ai14 mice, which express tdTomato upon Cre recombination (Figure 1). When the same lipid nanoparticles were formulated with mRNAs encoding fluorescent protein (GFP and tdTomato) and administered to wild-type mice, no fluorescence was observed above background *in vivo* for whole organs or individual cell populations (Figures 2, 4, and 5), which highlights the significantly improved sensitivity of the Cre/Ai14 model. It should be noted that the GFP, tdTomato, and Cre mRNAs used in these experiments are commercially available and differed only in their coding regions; they had identical 5′ caps, UTR sequences, poly(A) tail lengths, and base modifications, all of which are known to strongly influence the potency of the mRNA.[1] We found one report in the literature of measuring expression from GFP mRNA *in vivo* with flow cytometry,[13] but the GFP mRNA was delivered at far higher doses than we demonstrate (1 mg/kg versus as low as 0.01 mg/kg), and the GFP mRNA was also highly optimized and synthesized in-house.[42] Because both the Ai14 mice and the Cre mRNA are readily commercially available, the Ai14/Cre mRNA model would permit researchers without access to often proprietary mRNA optimization algorithms to screen mRNA vectors *in vivo* for the first time at far lower doses and with less potent delivery materials.

Applications of the Ai14/Cre mRNA Model

Although it has significant advantages, the Ai14/Cre mRNA model does have limitations compared with traditional FLuc models. Genetically engineered Ai14 mice are more expensive to purchase than standard C57BL/6 or other mouse strains, and FLuc mRNA remains a fast (luminescence visible minutes after substrate injection) and robust (low signal-to-noise ratio) method to screen mRNA expression in tissues *in vivo*. FLuc mRNA can also be non-invasive, making it appropriate for longitudinal studies to measure protein expression over time. Additionally, although FLuc expression (the output) in a given tissue should be directly proportional to the quantity of transfected mRNA (the input), the Ai14/Cre mRNA model is a binary "on/off" system, where the successful transfection of one Cre mRNA would have the same tdTomato expression as many Cre mRNAs. Thus, we envision the Ai14/Cre mRNA system to be used not as a

replacement of FLuc models but, rather, primarily for identifying transfected cell populations *in vivo* and discovering low-expressing tissues or rare cell types too weak to be visualized with FLuc. We also envision the system to be used for determining these hits at lower doses, longer time points, and with less overall efficacious vectors.

The binary nature of the Ai14/Cre mRNA mouse model can provide information difficult to observe using a simple FLuc system. For example, tdTomato expression following treatment with the LNP-2 formulation saturates around a dose of 0.1 to 0.3 mg/kg in the lungs (Figures 2E and 4B), suggesting that a certain number of endothelial cells might be incapable of transfection regardless of dose escalation. Additionally, a binary readout in which only one Cre protein (from delivered Cre mRNA) must transfect the nucleus to express tdTomato is highly analogous to genome editing applications such as the CRISPR/Cas system, in which one Cas9 protein (from delivered Cas9 mRNA) must transfect the nucleus to edit a gene. Thus, we anticipate the Ai14/Cre mRNA mouse model to be highly useful for researchers performing mechanistic analyses of *in vivo* mRNA delivery and for those studying *in vivo* genome editing with nuclease-encoding mRNAs. A recent publication further demonstrated the utility of reporter mice similar to Ai14 mice for CRISPR applications by co-delivering Cas9 mRNA and single guide RNA (sgRNA) against loxP, thus cutting out the STOP cassette and inducing tdTomato in transfected cells.[43]

Conclusions

In conclusion, we have demonstrated the use of a mouse model in which mRNA expression can be identified with single-cell resolution *in vivo*. Because of the increased sensitivity of the Ai14/Cre mRNA model over traditional reporter mRNAs (i.e., luciferase, GFP, or tdTomato), we discovered that a previously reported lipid nanoparticle mRNA formulation is capable of transfecting splenic lymphocytes and antigen-presenting cells, and we designed a new mRNA formulation capable of transfecting lung endothelial cells. We propose that this described Ai14/Cre mRNA mouse model be used together with traditional luciferase models in future experiments to screen and optimize mRNA delivery vectors for therapeutic applications, including protein replacement therapies, genomic engineering, and mRNA vaccines.

MATERIALS AND METHODS

mRNA

Commercially available mRNA encoding nuclear localization signal (NLS)-Cre and EGFP were purchased from TriLink Biotechnologies (San Diego, CA). mRNA encoding tdTomato was custom-synthesized by TriLink according to the same specifications as Cre and GFP. All mRNAs were 100% modified with pseudouridine and 5-methylcytidine, capped with Cap 0, and polyadenylated.

Lipid Nanoparticle Formulation

The ethanol phase contained a mixture of cKK-E12 (prepared as described previously,[30] courtesy of Shire Pharmaceuticals, Lexington, MA), 1,2-dioleoyl-*sn*-glycero-3-phosphoethanolamine (DOPE, Avanti Polar Lipids, Alabaster, AL), 1,2-dioleoyl-3-trimethylammonium-propane (DOTAP, Avanti), cholesterol (Sigma), and/or 1,2-dimyristoyl-*sn*-glycero-3-phosphoethanolamine-N-(methoxy[polyethylene glycol]-2000) (C14 PEG 2000, Avanti) in differing molar ratios (Table S1) for LNP-1 and LNP-2. The aqueous phase contained mRNA in 10 mM citrate buffer (pH 3). Syringe pumps were used to mix the ethanol and aqueous phases together at a 1:3 volume ratio in a microfluidic chip device as described previously.[44] The resulting LNPs were dialyzed against 1× PBS in a 20,000 molecular weight cutoff (MWCO) cassette at 4°C for 2 hr.

Lipid Nanoparticle Characterization

To calculate the mRNA encapsulation efficiency, a modified Quant-iT RiboGreen RNA assay (Invitrogen) was performed as described previously.[45] The diameter (measured by intensity) and polydispersity of the LNPs were measured using dynamic light scattering (ZetaPALS, Brookhaven Instruments). Zeta potential was measured using the same instrument in a 0.1× PBS solution.

Animal Experiments

Animal studies were approved by the Massachusetts Institute of Technology (MIT) Institutional Animal Care and Use Committee and were consistent with local, state, and federal regulations as applicable. Female B6.Cg-*Gt(ROSA)26Sor*$^{tm14(CAG\text{-}tdTomato)Hze}$/J (Ai14, stock no. 007914) mice and control C57BL/6 mice were purchased from Jackson Laboratory (Bar Harbor, ME). Mice (18–22 g) were intravenously injected with LNPs via the tail vein at a dose of 0.3 mg/kg, unless otherwise noted, for dose-response experiments. For GFP and tdTomato mRNA experiments, *in vivo* measurements were taken 24 hr post-injection (according to the half-life of the proteins). For Cre mRNA experiments, measurements were taken 48 hr post-injection. Mice were euthanized by carbon dioxide asphyxiation.

Whole-Organ Imaging

To measure whole-organ fluorescence, organs were collected and measured using an IVIS imaging system (PerkinElmer, Waltham, MA) and quantified using LivingImage software (PerkinElmer).

Two-Photon Excitation Microscopy

Imaging was performed on an FV-1000MPE microscope (Olympus America, Waltham MA) using a 25×, numerical aperture (N.A.) 1.05 water objective. Excitation was achieved using a DeepSee Tai-sapphire femtosecond pulse laser (Spectro-Physics, Santa Clara, CA) at 840 nm. The emitted fluorescence was collected by photomultiplier tubes (PMTs) with emission filters of 425/30 nm for collagen 1, 525/45 nm for tissue autofluorescence, and 607/70 nm for tdTomato. Collagen 1 was excited by second harmonic generation and emits as polarized light at half the excitation wavelength. All images were processed using ImageJ.

Flow Cytometry

Spleen single cell suspensions were prepared as described previously.[46] To prepare lung single-cell suspensions, lungs were digested in a mixture of collagenase I (450 U), collagenase XI (125 U), and

DNase I (2 U) in 1 mL at 37°C for 1 hr. The digest was passed through a 70-μm filter. Following centrifugation and removal of supernatant, cells were treated with red blood cell (RBC) lysis buffer for 10 min at 4°C and then passed through a 40-μm filter.

After single-cell suspensions were generated, cells were stained with a mixture of anti-mouse antibodies at 1:300 dilution in flow buffer (PBS containing 0.5% BSA and 2 mM EDTA). The antibodies included T cell receptor β (TCR-β, clone H57-597), CD19 (clone 6D5), CD11b (clone M1/70), Ly-6G (clone 1A8), CD45 (clone 30-F11), F4/80 (clone BM8), CD11c (clone N418), CD31 (clone 390), and EpCAM (clone G8.8). Antibodies were purchased from BioLegend (San Diego, CA), and data were collected using a BD LSR II cytometer (BD Biosciences). Data were analyzed with FlowJo software (Ashland, OR).

Splenic cell populations were identified as follows: T cells: $CD45^+$, $CD11b^-$, TCR-β^+; B cells: $CD45^+$, $CD11b^-$, $CD19^+$; neutrophils: $CD45^+$, $CD11b^+$, Ly-$6G^+$; macrophages: $CD45^+$, $CD11b^+$, F4/80^+; dendritic cells: $CD45^+$, $CD11b^+$, $CD11c^+$; other myeloid cells: $CD45^+$, $CD11b^+$, Ly-$6G^-$, F4/80^-, $CD11c^-$. Lung cell populations were identified as follows: endothelial cells, $CD31^+$; epithelial cells, $EpCAM^+$; immune cells, $CD45^+$.

In Vitro Experiments

HeLa cells (ATCC, Manassas, VA) were cultured in high-glucose DMEM (Thermo Fisher Scientific) supplemented with 10% fetal bovine serum. Cells were maintained at 37°C and 5% CO_2. Cells were plated at 20,000 cells/well in a clear-bottom, black-walled, 96-well plate. After 24 hr, the medium in each well was replaced with 150 μL of medium containing GFP or tdTomato mRNA-LNPs or mRNA-Stemfect complexes. The mRNA transfection reagent Stemfect (Stemgent, Lexington, MA) was used according to the manufacturer's protocol. After another 24 hr, the fluorescence was measured. Fluorescence microscopy was performed with an EVOS FL cell imaging system (Thermo Fisher Scientific). To quantify the fluorescence, cells were lysed with 50 μL of Cell Lytic M for 10 min at 37°C at 400 rpm. 150 μL of PBS was added to each well, and fluorescence was measured with a Tecan Infinite m200 Pro microplate reader.

Statistics

To compare two groups, a Student's t test was performed, assuming a Gaussian distribution with unequal variances. Statistical significance was defined with an alpha level of 0.05. All statistical analyses were performed using GraphPad Prism 7 software (La Jolla, CA).

SUPPLEMENTAL INFORMATION

Supplemental Information includes six figures and one table and can be found with this article online at https://doi.org/10.1016/j.omtn.2017.11.005.

AUTHOR CONTRIBUTIONS

K.J.K., M.A.O., J.R.D., R.L., A.J., and D.G.A. designed the experiments, which were performed by K.J.K., M.A.O., J.E.H., S.B., and J.W. K.J.K., M.A.O., J.C.K., R.L., A.J., and D.G.A. prepared the manuscript, which was read and approved by all authors prior to submission.

ACKNOWLEDGMENTS

This work was supported by Shire Pharmaceuticals (Lexington, MA), the Koch Institute Marble Center for Cancer Medicine, and Cancer Center Support (Core) grant P30-CA14051. We thank the Animal Imaging and Preclinical Testing Core, Microscopy, and Flow Cytometry Core at the Koch Institute at MIT.

REFERENCES

1. Sahin, U., Karikó, K., and Türeci, Ö. (2014). mRNA-based therapeutics–developing a new class of drugs. Nat. Rev. Drug Discov. *13*, 759–780.
2. Sergeeva, O.V., Koteliansky, V.E., and Zatsepin, T.S. (2016). mRNA Based Therapeutics – Advances and Perspectives. Biochemistry *81*, 709–722.
3. Kauffman, K.J., Webber, M.J., and Anderson, D.G. (2016). Materials for non-viral intracellular delivery of messenger RNA therapeutics. J. Control. Release *240*, 227–234.
4. Yin, H., Kanasty, R.L., Eltoukhy, A.A., Vegas, A.J., Dorkin, J.R., and Anderson, D.G. (2014). Non-viral vectors for gene-based therapy. Nat. Rev. Genet. *15*, 541–555.
5. Tolmachov, O.E., and Tolmachova, T. (2015). Design and Production of mRNA-based Gene Vectors for Therapeutic Reprogramming of Cell Fate. Gene Technol. *4*, e117.
6. Pollard, C., De Koker, S., Saelens, X., Vanham, G., and Grooten, J. (2013). Challenges and advances towards the rational design of mRNA vaccines. Trends Mol. Med. *19*, 705–713.
7. Reichmuth, A.M., Oberli, M.A., Jeklenec, A., Langer, R., and Blankschtein, D. (2016). mRNA vaccine delivery using lipid nanoparticles. Ther. Deliv. *7*, 319–334.
8. Kim, N., Duncan, G.A., Hanes, J., and Suk, J.S. (2016). Barriers to inhaled gene therapy of obstructive lung diseases: A review. J. Control. Release *240*, 465–488.
9. Bangel-Ruland, N., Tomczak, K., Fernández Fernández, E., Leier, G., Leciejewski, B., Rudolph, C., Rosenecker, J., and Weber, W.M. (2013). Cystic fibrosis transmembrane conductance regulator-mRNA delivery: a novel alternative for cystic fibrosis gene therapy. J. Gene Med. *15*, 414–426.
10. Fenton, O.S., Kauffman, K.J., McClellan, R.L., Appel, E.A., Dorkin, J.R., Tibbitt, M.W., Heartlein, M.W., DeRosa, F., Langer, R., and Anderson, D.G. (2016). Bioinspired Alkenyl Amino Alcohol Ionizable Lipid Materials for Highly Potent In Vivo mRNA Delivery. Adv. Mater. *28*, 2939–2943.
11. Kauffman, K.J., Dorkin, J.R., Yang, J.H., Heartlein, M.W., DeRosa, F., Mir, F.F., Fenton, O.S., and Anderson, D.G. (2015). Optimization of Lipid Nanoparticle Formulations for mRNA Delivery in Vivo with Fractional Factorial and Definitive Screening Designs. Nano Lett. *15*, 7300–7306.
12. Karikó, K., Muramatsu, H., Welsh, F.A., Ludwig, J., Kato, H., Akira, S., and Weissman, D. (2008). Incorporation of pseudouridine into mRNA yields superior nonimmunogenic vector with increased translational capacity and biological stability. Mol. Ther. *16*, 1833–1840.
13. Kranz, L.M., Diken, M., Haas, H., Kreiter, S., Loquai, C., Reuter, K.C., Meng, M., Fritz, D., Vascotto, F., Hefesha, H., et al. (2016). Systemic RNA delivery to dendritic cells exploits antiviral defence for cancer immunotherapy. Nature *534*, 396–401.
14. Kaczmarek, J.C., Patel, A.K., Kauffman, K.J., Fenton, O.S., Webber, M.J., Heartlein, M.W., DeRosa, F., and Anderson, D.G. (2016). Polymer-Lipid Nanoparticles for Systemic Delivery of mRNA to the Lungs. Angew. Chem. Int. Ed. Engl. *55*, 13808–13812.
15. Oberli, M.A., Reichmuth, A.M., Dorkin, J.R., Mitchell, M.J., Fenton, O.S., Jaklenec, A., Anderson, D.G., Langer, R., and Blankschtein, D. (2017). Lipid Nanoparticle Assisted mRNA Delivery for Potent Cancer Immunotherapy. Nano Lett. *17*, 1326–1335.
16. Andries, O., Mc Cafferty, S., De Smedt, S.C., Weiss, R., Sanders, N.N., and Kitada, T. (2015). N(1)-methylpseudouridine-incorporated mRNA outperforms pseudouridine-incorporated mRNA by providing enhanced protein expression and reduced immunogenicity in mammalian cell lines and mice. J. Control. Release *217*, 337–344.

17. Pardi, N., Tuyishime, S., Muramatsu, H., Kariko, K., Mui, B.L., Tam, Y.K., Madden, T.D., Hope, M.J., and Weissman, D. (2015). Expression kinetics of nucleoside-modified mRNA delivered in lipid nanoparticles to mice by various routes. J. Control. Release *217*, 345–351.

18. Wang, Y., Su, H.-H., Yang, Y., Hu, Y., Zhang, L., Blancafort, P., and Huang, L. (2013). Systemic delivery of modified mRNA encoding herpes simplex virus 1 thymidine kinase for targeted cancer gene therapy. Mol. Ther. *21*, 358–367.

19. Adams, S.T., Jr., and Miller, S.C. (2014). Beyond D-luciferin: expanding the scope of bioluminescence imaging in vivo. Curr. Opin. Chem. Biol. *21*, 112–120.

20. Prescher, J.A., and Contag, C.H. (2010). Guided by the light: visualizing biomolecular processes in living animals with bioluminescence. Curr. Opin. Chem. Biol. *14*, 80–89.

21. Hoshino, H., Nakajima, Y., and Ohmiya, Y. (2007). Luciferase-YFP fusion tag with enhanced emission for single-cell luminescence imaging. Nat. Methods *4*, 637–639.

22. Saito, K., Chang, Y.-F., Horikawa, K., Hatsugai, N., Higuchi, Y., Hashida, M., Yoshida, Y., Matsuda, T., Arai, Y., and Nagai, T. (2012). Luminescent proteins for high-speed single-cell and whole-body imaging. Nat. Commun. *3*, 1262.

23. Kormann, M.S.D., Hasenpusch, G., Aneja, M.K., Nica, G., Flemmer, A.W., Herber-Jonat, S., Huppmann, M., Mays, L.E., Illenyi, M., Schams, A., et al. (2011). Expression of therapeutic proteins after delivery of chemically modified mRNA in mice. Nat. Biotechnol. *29*, 154–157.

24. Ishikawa, T.O., and Herschman, H.R. (2011). Conditional bicistronic Cre reporter line expressing both firefly luciferase and β-galactosidase. Mol. Imaging Biol. *13*, 284–292.

25. Wang, Y., Sun, Z., Peng, J., and Zhan, L. (2007). Bioluminescent imaging of hepatocellular carcinoma in live mice. Biotechnol. Lett. *29*, 1665–1670.

26. Madisen, L., Zwingman, T.A., Sunkin, S.M., Oh, S.W., Zariwala, H.A., Gu, H., Ng, L.L., Palmiter, R.D., Hawrylycz, M.J., Jones, A.R., et al. (2010). A robust and high-throughput Cre reporting and characterization system for the whole mouse brain. Nat. Neurosci. *13*, 133–140.

27. Snapp, E.L. (2009). Fluorescent proteins: a cell biologist's user guide. Trends Cell Biol. *19*, 649–655.

28. Rubart, M. (2004). Two-photon microscopy of cells and tissue. Circ. Res. *95*, 1154–1166.

29. Baratta, J.L., Ngo, A., Lopez, B., Kasabwalla, N., Longmuir, K.J., and Robertson, R.T. (2009). Cellular organization of normal mouse liver: a histological, quantitative immunocytochemical, and fine structural analysis. Histochem. Cell Biol. *131*, 713–726.

30. Dong, Y., Love, K.T., Dorkin, J.R., Sirirungruang, S., Zhang, Y., Chen, D., Bogorad, R.L., Yin, H., Chen, Y., Vegas, A.J., et al. (2014). Lipopeptide nanoparticles for potent and selective siRNA delivery in rodents and nonhuman primates. Proc. Natl. Acad. Sci. USA *111*, 3955–3960.

31. Dahlman, J.E., Barnes, C., Khan, O., Thiriot, A., Jhunjunwala, S., Shaw, T.E., Xing, Y., Sager, H.B., Sahay, G., Speciner, L., et al. (2014). In vivo endothelial siRNA delivery using polymeric nanoparticles with low molecular weight. Nat. Nanotechnol. *9*, 648–655.

32. Khan, O.F., Zaia, E.W., Jhunjhunwala, S., Xue, W., Cai, W., Yun, D.S., Barnes, C.M., Dahlman, J.E., Dong, Y., Pelet, J.M., et al. (2015). Dendrimer-inspired nanomaterials for the in vivo delivery of siRNA to lung vasculature. Nano Lett. *15*, 3008–3016.

33. Budhiraja, R., Tuder, R.M., and Hassoun, P.M. (2004). Endothelial dysfunction in pulmonary hypertension. Circulation *109*, 159–165.

34. Dudley, A.C. (2012). Tumor endothelial cells. Cold Spring Harb. Perspect. Med. *2*, a006536.

35. Bronte, V., and Pittet, M.J. (2013). The spleen in local and systemic regulation of immunity. Immunity *39*, 806–818.

36. Love, K.T., Mahon, K.P., Levins, C.G., Whitehead, K.A., Querbes, W., Dorkin, J.R., Qin, J., Cantley, W., Qin, L.L., Racie, T., et al. (2010). Lipid-like materials for low-dose, in vivo gene silencing. Proc. Natl. Acad. Sci. USA *107*, 1864–1869.

37. Semple, S.C., Akinc, A., Chen, J., Sandhu, A.P., Mui, B.L., Cho, C.K., Sah, D.W., Stebbing, D., Crosley, E.J., Yaworski, E., et al. (2010). Rational design of cationic lipids for siRNA delivery. Nat. Biotechnol. *28*, 172–176.

38. Schrom, E., Huber, M., Aneja, M., Dohmen, C., Emrich, D., Geiger, J., Hasenpusch, G., Herrmann-Janson, A., Kretzschmann, V., Mykhailyk, O., et al. (2017). Translation of Angiotensin-Converting Enzyme 2 upon Liver- and Lung-Targeted Delivery of Optimized Chemically Modified mRNA. Mol. Ther. Nucleic Acids *7*, 350–365.

39. Broos, K., Van der Jeught, K., Puttemans, J., Goyvaerts, C., Heirman, C., Dewitte, H., Verbeke, R., Lentacker, I., Thielemans, K., and Breckpot, K. (2016). Particle-mediated Intravenous Delivery of Antigen mRNA Results in Strong Antigen-specific T-cell Responses Despite the Induction of Type I Interferon. Mol. Ther. Nucleic Acids *5*, e326.

40. Park, J., Park, J., Pei, Y., Xu, J., and Yeo, Y. (2016). Pharmacokinetics and biodistribution of recently-developed siRNA nanomedicines. Adv. Drug Deliv. Rev. *104*, 93–109.

41. Whitehead, K.A., Dorkin, J.R., Vegas, A.J., Chang, P.H., Veiseh, O., Matthews, J., Fenton, O.S., Zhang, Y., Olejnik, K.T., Yesilyurt, V., et al. (2014). Degradable lipid nanoparticles with predictable in vivo siRNA delivery activity. Nat. Commun *5*, 4277.

42. Holtkamp, S., Kreiter, S., Selmi, A., Simon, P., Koslowski, M., Huber, C., Türeci, O., and Sahin, U. (2006). Modification of antigen-encoding RNA increases stability, translational efficacy, and T-cell stimulatory capacity of dendritic cells. Blood *108*, 4009–4017.

43. Miller, J.B., Zhang, S., Kos, P., Xiong, H., Zhou, K., Perelman, S.S., Zhu, H., and Siegwart, D.J. (2017). Non-viral CRISPR/Cas gene editing in vitro and in vivo enabled by synthetic nanoparticle co-delivery of Cas9 mRNA and sgRNA. Angew. Chem. Int. Ed. Engl. *56*, 1059–1063.

44. Chen, D., Love, K.T., Chen, Y., Eltoukhy, A.A., Kastrup, C., Sahay, G., Jeon, A., Dong, Y., Whitehead, K.A., and Anderson, D.G. (2012). Rapid discovery of potent siRNA-containing lipid nanoparticles enabled by controlled microfluidic formulation. J. Am. Chem. Soc. *134*, 6948–6951.

45. Heyes, J., Palmer, L., Bremner, K., and MacLachlan, I. (2005). Cationic lipid saturation influences intracellular delivery of encapsulated nucleic acids. J. Control. Release *107*, 276–287.

46. Kauffman, K.J., Mir, F.F., Jhunjhunwala, S., Kaczmarek, J.C., Hurtado, J.E., Yang, J.H., Webber, M.J., Kowalski, P.S., Heartlein, M.W., DeRosa, F., and Anderson, D.G. (2016). Efficacy and immunogenicity of unmodified and pseudouridine-modified mRNA delivered systemically with lipid nanoparticles in vivo. Biomaterials *109*, 78–87.